Nanosized Porphyrin J-Aggregates in Water/AOT/Decane Microemulsions

Maria Angela Castriciano,[†] Andrea Romeo,[†,‡] Valentina Villari,[§] Norberto Micali,[§] and Luigi Monsù Scolaro*,[†,‡]

Dipartimento di Chimica Inorganica, Chimica Analitica e Chimica Fisica, Università di Messina, Salita Sperone 31, 98166 Vill.S.Agata, Messina, Italy, INFM, Unità di Messina, Messina, Italy, and CNR - Istituto per i Processi Chimico-Fisici, sez. Messina, Via La Farina 237, 98123, Messina, Italy

Received: March 23, 2004; In Final Form: April 26, 2004

Water/decane/AOT microemulsions have been used to obtain J-aggregates of the anionic water soluble porphyrin tetrakis(4-sulfonatophenyl)porphyrin (TPPS$_4$), having sizes that are controlled by the dimension of the water pool. The kinetics of aggregation have been investigated on changing pH, ionic strength and size of the microemulsions and treated by a model derived for self-assembling processes and based on the catalytic role of a critical size nucleus. The analysis of the present data evidences the role of dimer or trimer in the rate determining step. The J-aggregates exhibit resonance light scattering (RLS) signals whose intensities follow a behavior that is predicted from the quantum mechanical theory developed for RLS. Depolarized light scattering together with quasielastic light scattering experiments allow for an estimation of the geometrical arrangement of the porphyrin linear arrays inside the microemulsions and the corresponding aggregation number. The ratio between the coherence length and the hydrodynamic radius of the aggregates decreases on increasing the size of the water pool, being close to the unity for the smaller nanoaggregates.

Introduction

The amazing recent progress in nanotechnology is due largely to the capability to synthesize, explore, and exploit materials at the nanometer scale. From a fundamental point of view, nanostructures are interesting because they exhibit unusual optical and optoelectronic properties, often quite different from those of single molecules or the bulk material.[1] In this respect, porphyrins are attractive compounds because they are relatively easy to synthesize and their photophysical properties can be tuned through careful choice of peripheral substituent groups and inserted metal ions.[2] In particular, water soluble porphyrins are very interesting because their self-aggregation can be conveniently controlled by screening the charge repulsion through the ionic strength and pH.[3]

During the past decade, J-aggregates formed by porphyrins have attracted the interest of several research groups, due to their peculiar structural and photophysical properties,[4−6] which makes them potential candidates for applications in nonlinear optics, nanometer-sized photoconductors, and light harvesting systems. In particular, the diacid form of the water-soluble tetrakis(4-sulfonatophenyl)porphyrin (TPPS$_4$), under highly acidic conditions (usually at pH < 1) and/or in the presence of cationic species[7−16] and templating reagents,[17,18] leads to such aggregates, characterized by a very narrow and red-shifted J-band (at 489 nm, $\Delta\lambda = +55$ nm), exhibiting a large resonant enhancement of the scattered light.[11,19] The structure is stabilized through a network of hydrogen bonds acting between the anionic sulfonate groups and the charged protonated nitrogen atoms. Recent reports have pointed out the presence in solution of rod-like nanoaggregates,[20,21] whose coherence length and size can be controlled by a proper choice of the nucleating agent. These properties of the J-aggregates are expected to play an important role in determining nonlinear optical effects.[22] On the other hand, the involvement of a quite large number of porphyrin units ($N \sim 10^4-10^5$) in the aggregates has been addressed also by previous light scattering experiments, which have also pointed out the presence of an extremely weak network in solution whose structure can be described in terms of fractal geometry.[23,24]

The use of microemulsions as nanoreactors to synthesize and control the size of nanoparticles is well established,[25] and the interactions of several water-soluble porphyrins have been investigated.[26−28] Here we report on the aggregation of TPPS$_4$ porphyrin in sodium bis(2-ethylhexyl)solfosuccinate (AOT)/decane/water ternary system, leading to J-aggregates under mildly acidic conditions (pH $\sim$ 3) whose size is controlled by the dimensions of the water pool inside microemulsions. This ternary system has been selected (i) because its behavior is well known[29−32] and (ii) to minimize the interaction of the anionic porphyrin with the anionic surfactant. The dimension imposed by the water pool in which the porphyrins are confined is expected to control and limit the growth of J-aggregates, allowing for a better matching between the coherence length and the physical size of these species.

Experimental Section

The porphyrin *meso*-tetrakis(4-sulfonatophenyl)porphyrin was purchased from Aldrich Co. as tetrasodium salt. Aqueous stock solutions of this porphyrin (80 μM) were prepared in dust-free Millipore water, stored in the dark, and used within a day of preparation. High purity AOT (Fluka, 99%) and decane (Aldrich, spectrophotometric grade) were used as received.

Microemulsions were prepared by mixing the proper quantities of AOT, decane, and water and equilibrated for at least a week. The volume fraction ϕ was kept at 0.05. The ratio $w_0 = $ [water]/[AOT] was changed in the range 5−65. As pointed out

* Corresponding author. Tel.: +39 090 6765711, Fax: +39 090 393756, e-mail: monsu@chem.unime.it
† Università di Messina.
‡ INFM.
§ CNR - Istituto per i Processi Chimico-Fisici.

Nanosized Porphyrin J-Aggregates

J. Phys. Chem. B, Vol. 108, No. 26, 2004 **9055**

below, aggregation occurred only for $w_0 \geq 32$, and it was achieved by mixing equal volumes of microemulsions containing concentrated porphyrin in water (80 μM) and citrate buffer at the selected pH and ionic strength. The effective hydrodynamic radii were measured before mixing and after reaching equilibrium. In all the cases, except $w_0 = 65$, we found that the dimensions do not change and correspond to those obtained for microemulsions containing only water at each w_0. This finding points to the fact that aggregates are effectively confined to the water pool. The only observed discrepancy is likely attributed to the limiting value of w_0 in the phase diagram for a droplet microemulsion.

UV/vis spectra were carried out on a Hewlett-Packard model 8453 diode array spectrophotometer using 1 cm path length quartz cells. Resonance light scattering (RLS) experiments were performed on a Jasco model FP-750 spectrofluorimeter, adopting a synchronous scan protocol with a right angle geometry. RLS spectra were not corrected for the absorption of the samples. Depolarized resonance light scattering measurements were obtained on the same instrument equipped with linear polarizers (Sterling Optics 105UV). The depolarization ratio is defined as $\rho_V(90) = I_{VH}/I_{VV}$, where I_{VH} and I_{VV} are the scattered light intensities with horizontal and vertical polarization, respectively. The different transmission efficiency of polarized light by both excitation and emission monochromators has been accounted for by correcting the I_{VH} value through the equation $\rho_V(90) = G \times I_{VH}/I_{VV}$, where $G = I_{HV}/I_{HH}$ is a correction factor.[33] Quasi-elastic light scattering (QELS) measurements were performed by using an experimental setup based on a Malvern 4700 submicron particle analyzer system and a 20 mW polarized Nd:YAG laser (532 nm) to probe the sample.

Kinetic experiments were carried out in the thermostated compartment of the spectrophotometer using a Hellma cell with two chambers filled by equal volumes of buffer and porphyrin in microemulsions. The kinetic runs were started by simply turning the cell upside down. The analysis of the kinetic profiles has been performed by a nonlinear best fitting procedure of the extinction data (collected at 490 nm) to eq 1, which is the integrated form of eq 2 (see the section *Kinetics of the Aggregation Process*):

$$\text{Ext} = \text{Ext}_\infty + (\text{Ext}_0 - \text{Ext}_\infty)\,(1 + (m-1)\{k_0 t + (n+1)^{-1}$$
$$(k_c\, t)^{n+1}\})^{-1/(m-1)} \quad (1)$$

with Ext_0, Ext_∞, k_0, k_c, m, and n as the parameters to be optimized (Ext, Ext_0 and Ext_∞ are the extinction at time t, at $t = 0$, and the end of aggregation, respectively). The kinetic data were analyzed by using the software package Origin v 6.0 (Microcal, 1999).

Results and Discussion

At neutral pH, various species are present in the water pool of the microemulsions as probed by UV−vis spectroscopy. The main component exhibits a Soret band at 414 nm that can be safely attributed to the monomeric neutral porphyrin, which is noninteracting with the inner polar headgroups of the anionic surfactant, due to electrostatic repulsion. On mixing equal volumes of TPPS$_4$ and citrate buffer in microemulsions, two different patterns of behavior are observed, depending on the w_0 ratio: (i) for $w_0 < 32$, the UV−vis spectra do not change, even after a month, indicating the absence of aggregation; (ii) for $w_0 \geq 32$, on mixing the microemulsions, the UV−vis spectra show an almost instantaneous formation of a species with a Soret band at 434 nm and two less intense Q-bands at 594 and
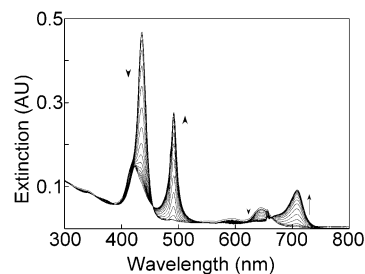
Figure 1. UV−vis spectral changes with time on mixing TPPS$_4$ (40 μM) with 25 mM citrate buffer at pH 2.7 in microemulsions ($w_0 = 65$, $T = 293$ K, scanning time 100 s).
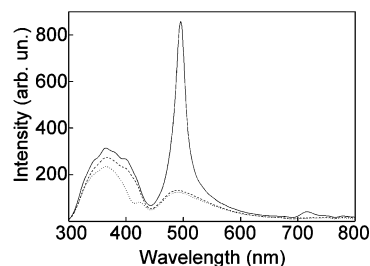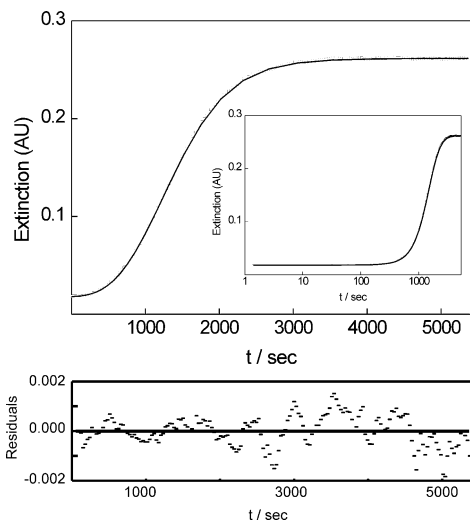

Figure 2. RLS spectra of 25 mM citrate buffer pH 2.7 (dashed line), TPPS$_4$ (40 μM in water, dotted line), and TPPS$_4$ J-aggregate ($w_0 = 65$, $T = 293$ K, solid line). The apparent well at 440 nm is due to the instrumental transfer function of both excitation and emission monochromators.

648 nm, which slowly interconverts to a final species with a narrow peak located at 490 nm, a broader one at 424 nm and a series of three Q-bands at 637, 671, and 709 nm (Figure 1).

According to the monomeric nature of the initial species, the RLS spectra of the starting solutions evidence profiles due to normal Rayleigh scattering coming from the microemulsions, and additional wells at 414 nm due to photon loss for absorption (Soret band). On the contrary, the RLS spectra of the final mixtures show an intense and sharp peak at 500 nm, indicating the presence of aggregated porphyrins (Figure 2). On the basis of these spectroscopic features, we can attribute the initial transient species to the diacid zwitterionic porphyrin and the final species to the J-aggregated TPPS$_4$ inside the microemulsion water pool. From UV−vis spectroscopy, QELS, and optical microscopy (that does not show the formation of any precipitate), we can conclude that the J-aggregates are confined to the microemulsions and are stable for months.[34]

Kinetics of the Aggregation Process. The formation of TPPS$_4$ J-aggregates inside the microemulsions follows a sigmoidal profile, which is characterized by the presence of an induction or lag-time at the beginning of the process (Figure 3). This pattern of behavior is very similar to what was already observed for the same aggregation process in acidic aqueous solutions.[23,35] To get insight into the aggregation process, we have carried out kinetic experiments as a function of w_0, pH, and ionic strength of the citrate buffer. The analysis of the kinetic traces has been performed through a nonconventional approach that has been proved to be successful in treating the formation of J-aggregates and the autocatalyzed organization of cationic porphyrins on nucleic acid templates.[35,36] In such a model, the rate determining step for the aggregation is the formation of a "critical size" assembly which catalyzes the further growth. The reported rate law is given by the following expression:

$$-\frac{d[M]}{dt} = k(t)\left\{\frac{([M]-[M]_e)^m}{([M]_0-[M]_e)^{m-1}}\right\} \quad (2)$$

9056 *J. Phys. Chem. B, Vol. 108, No. 26, 2004*

Castriciano et al.

Figure 3. UV−vis kinetic profile on mixing TPPS$_4$ (40 μM) with 25 mM citrate buffer at pH 2.7 in microemulsions ($w_0 = 65$, $\lambda = 490$ nm, $T = 293$ K). The solid line is the best-fitting of the experimental data with eq 1 (see text). The inset reports a linear-logarithmic plot of the same kinetic trace. The lower plot shows the residuals for the fitting procedure (180 data points, $R^2 = 0.99995$, $\chi^2 = 3.7 \times 10^{-7}$).

TABLE 1: Kinetic Parameters k_0, k_c, m, and n for the Aggregation of TPPS$_4$ in AOT/Water/Decane Microemulsions as Function of w_0, pH, and Ionic Strength ([TPPS$_4$] = 40 μM, $T = 293$ K)

	$10^5\,k_0$ (s^{-1})	$10^3\,k_c$ (s^{-1})	m	n
$w_0{}^a$				
32		1.36 ± 0.01	1.58 ± 0.02	1.11 ± 0.02
34		3.71 ± 0.03	2.53 ± 0.06	1.32 ± 0.04
43		5.36 ± 0.04	2.48 ± 0.04	1.15 ± 0.03
54	6.1 ± 0.2	1.09 ± 0.01	1.81 ± 0.02	3.85 ± 0.03
65	10.1 ± 0.3	1.46 ± 0.01	1.33 ± 0.01	1.43 ± 0.02
pH^b				
2.7	10.1 ± 0.3	1.46 ± 0.01	1.33 ± 0.01	1.43 ± 0.02
3.0	-	1.28 ± 0.02	2.06 ± 0.09	0.65 ± 0.04
3.3	6.9 ± 0.1	0.52 ± 0.01	1.49 ± 0.04	2.58 ± 0.08
3.5		0.20 ± 0.01	0.88 ± 0.02	1.40 ± 0.03
μ (mM)^c				
15	1.0 ± 0.1	1.18 ± 0.01	1.24 ± 0.01	1.45 ± 0.02
20		2.16 ± 0.01	1.37 ± 0.01	1.08 ± 0.01
25	10.1 ± 0.3	1.46 ± 0.01	1.33 ± 0.01	1.43 ± 0.02
30		3.79 ± 0.05	1.95 ± 0.05	0.77 ± 0.02
45		3.36 ± 0.05	2.23 ± 0.06	0.34 ± 0.01
50		4.66 ± 0.13	3.05 ± 0.16	0.48 ± 0.04

^{a} 25 mM citrate buffer at pH 2.7. ^{b} 25 mM citrate buffer, $w_0 = 65$. ^{c} citrate buffer at pH 2.7, $w_0 = 65$.

where m is an index related to the number of monomers in the initial assembly, $[M]$, $[M]_0$, and $[M]_e$ are the concentrations of porphyrin (expressed in terms of monomeric units) at time t, at the beginning, and at the end of the kinetic process, respectively. Assuming autocatalysis to be operative, the rate constant $k(t)$ is also time dependent, and it can be expressed as $k(t) = k_0 + k_c(k_c t)^n$. The rate constant k_0 (s^{-1}) governs the uncatalyzed process, while the constant k_c (s^{-1}) controls the autocatalytic pathway. The exponent n has been introduced from the theory developed for self-similar aggregation, in which the size of the aggregates scales with the time according to a power law.[37] Figure 3 reports a typical kinetic trace ($w_0 = 65$, pH = 2.7, in citrate buffer 25 mM at $T = 293$ K, $\lambda = 490$ nm) together with the best fitting analysis according to eq 1, which is the integrated form of eq 2. The quality of the fitting procedure is very high ($R^2 = 0.99995$) and, as already reported by Pasternack et al., this model allows to treat a complete kinetic profile without parsing the data into different sets.[35] Table 1 collects the kinetic parameters derived under different experimental conditions. An inspection of this table reveals that the values of the rate constant k_c exhibit a decrease on increasing the pH and decreasing the ionic strength of the buffering solution. This behavior is in line with what has been observed in aqueous solutions and can be explained in terms of the screening effects of the added salts on the electrostatic interactions between the zwitterionic diacid porphyrins into the J-aggregate.[23] In general the values of k_0, the rate constant for the uncatalyzed pathway, are in the range 10^{-5}–10^{-6} s^{-1}, an order of magnitude less than the corresponding rate constant k_c for the catalyzed pathway. In many cases, these values were so small that the fitting procedure gave virtually the same parameter set on fixing the k_0 value to zero. It is interesting to note that the mean values of both k_0 and k_c are very similar to those reported in the literature in the case of aggregation of TPPS$_4$ in aqueous acidic conditions ([TPPS$_4$] = 2.7–7.2 μM, pH = 0.5, $T = 298$ K).[35] This observation is in line with the expected higher rate of microemulsion exchange[38] in comparison with the porphyrin aggregation rates. The values of both m (0.9–3.5) and n (0.3–3.9) are considerably lower with respect to same parameters measured in bulk conditions ($m \approx 5$–6, $n \approx 8$).[35] These results suggest that a dimer or trimer should be the critical nucleus in the growth of TPPS$_4$

J-aggregates in the confined space of the microemulsion. The relevant difference with the parameter n could be again explained by the confinement of porphyrins into the water pools, leading to a consistently different power law for the growth of the clusters, with respect to the situation observed in bulk. A similar pattern of behavior has already been observed for the aggregation kinetics of chlorophyll a in aqueous solutions to form polymeric or "micellar aggregates" ($m \approx 1.8$, $n \approx 1.3$).[39]

Resonance Light Scattering Investigations. According to the theory of RLS, the scattering cross-section C_{sca} depends on the number N of interacting chromophores, being small and relatively constant for low N values, but steeply increasing after a threshold value of about 25 monomers.[33] The calculation of the scattering cross-section for a J-aggregate as a function of the number N of monomers has been performed according to the point dipole approximation as described in the literature.[33] Accordingly, we considered each monomer as described by a single transition moment μ_{mon} and frequency ν_{mon} (in cm^{-1}). When the slip angle between transition moments is $\varphi = 0$, the transition frequencies ν_m and the transition moments μ_m for the mth exciton state are given by the two following equations:

$$\nu_m = \nu_{mon} + 2\beta\cos\left(\frac{m\pi}{N+1}\right) \qquad (3)$$

$$\mu_m = \left(\frac{2}{N+1}\right)^{1/2}\sum_n \mu_{mon}\sin\left(\frac{mn\pi}{N+1}\right) \qquad (4)$$

where the sum is extended to all the N exciton coupled states in the aggregate. Equations 3 and 4 have been derived under the assumption that only nearest-neighbor interactions contribute to the exciton coupling constant β:

$$\beta = \frac{|\mu_{mon}|^2}{4\pi\epsilon_0\eta^2 R^3}(1 - 3\cos\theta) \qquad (5)$$

where ϵ_0 is the permittivity of free space, η is the refractive index of the medium, R is the distance, and θ is the angle between transition moment vectors in the aggregate.

The scattering cross-section C_{sca} is given by the following equation:

Nanosized Porphyrin J-Aggregates

J. Phys. Chem. B, Vol. 108, No. 26, 2004 **9057**

$$C_{\text{sca}} = \frac{8}{3}\pi^3\nu^4[\text{Re}(\alpha)^2 + \text{Im}(\alpha)^2] \qquad (6)$$

Assuming a system in which the dipole moment vector has one component, the quantum mechanical expressions for the real and imaginary parts of polarizability $\alpha(\nu)$ are given by

$$\text{Re}\alpha(\nu) = \frac{1}{2\pi\epsilon_0 hc}\sum_m \frac{(\nu_m^2 - \nu^2)\nu_m}{(\nu_m^2 - \nu^2)^2 + \nu^2\Gamma_m^2}|\mu_m|^2 \qquad (7)$$

$$\text{Im}\,\alpha(\nu) = \frac{1}{2\pi\epsilon_0 hc}\sum_m \frac{\nu\nu_m\Gamma_m}{(\nu_m^2 - \nu^2)^2 + \nu^2\Gamma_m^2}|\mu_m|^2 \qquad (8)$$

with Γ_m being the spectral line width. For the actual calculation of the scattering cross-section we choose monomer parameters that correspond to the Soret band of the diacid porphyrin ($\lambda_{\text{mon}} = 434$ nm, $\mu_{\text{mon}} = 4.3$ D). In the case of a J-aggregate, assuming a lateral arrangement of the transition moments with a slip angle φ (in the case of this linear aggregate, the angle θ between transition moment vectors is zero), the exciton theory predicts a negative value for the exciton coupling constant β, which is responsible for the observed red-shift of the Soret band with respect to the monomer. In the present case, considering the position of the J-band we have calculated $\beta = -1275$ cm^{-1}. Figure 4 shows the dependence of the measured RLS intensities of the J-aggregates (normalized and corrected for the corresponding extinction) on the number N derived from the hydrodynamic radii of the microemulsions (see below). It is interesting to note that the observed behavior is in very good agreement with the theoretical model.

In contrast to the scattering cross-section, which is strongly dependent on the size of the aggregate, the value of the depolarization ratio, $\rho_V(90)$, is related only to the principal values of the polarizability tensor at the resonance wavelength. As a consequence, the value of $\rho_V(90)$ can be conveniently used to gain information on the geometry of the excited state of an aggregated species. These values together with the experimental hydrodynamic radii and the calculated slip angles are reported in Table 2. Depolarized RLS measurements gave $\rho_V(90)$ ranging between 0.131 and 0.235, for the w_0 values 32 and 65, respectively. Assuming a parallel arrangement of the transition moments of the exciton-coupled chromophores and applying this simple model,[33] we have calculated the slip angle φ between adjacent porphyrin planes. On considering the lowest $\rho_V(90)$ value we estimate an angle $\varphi \approx 42°$, which decreases to $\varphi \approx 25°$ on increasing the microemulsion dimension. Interestingly, a decrease of the angle φ between the transition moments corresponds to an increase of the microemulsion radius, suggesting a gradual structural rearrangement of the J-aggregate.

The experimental findings allow us to propose a model for the structure of the TPPS$_4$ J-aggregates inside the microemulsions. On considering that the aggregates grow in the water pool and the dimensions are limited by the confined environment, it is possible to combine the estimated angles with simple geometrical analysis. The mean distance between adjacent porphyrin planes has been fixed to 3.5 Å, a value that is generally found in crystallographic determinations.[40] The arrangement of porphyrins is reported in Figure 5 and the calculation has been performed in the range $w_0 = 32-65$.

The experimental hydrodynamic radii have been corrected for the size of a single AOT molecule (15 Å), obtaining diameter values between 106 and 310 Å. Assuming that the lateral arrangement determines the major dimension (length) of the
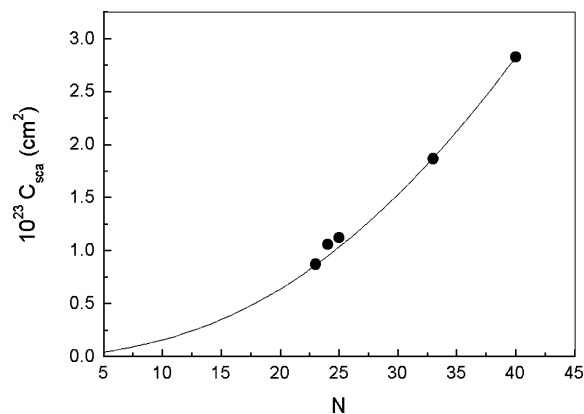
Figure 4. Theoretical dependence of scattering cross-section for J-aggregates as function of the aggregation number N (solid line, calculated according ref 33 for $\lambda_{\text{mon}} = 434$ nm, $\mu_{\text{mon}} = 4.3$ D, $\beta = -1275$ cm^{-1}). RLS experimental intensity (circles) corresponding to J-aggregates in microemulsions ($w_0 = 32-65$) are normalized and corrected for extinction of the samples and linearly corrected to fit the theoretical scattering cross-section; the corresponding N values have been evaluated from the hydrodynamic radii of the microemulsions and geometrical consideration (see text).
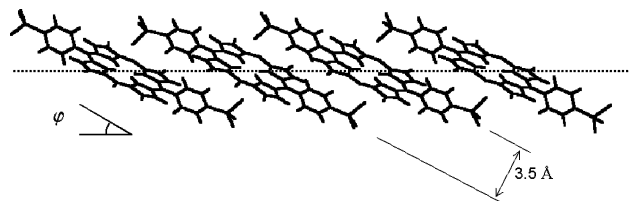
Figure 5. Molecular model of the arrangement of porphyrin units into a J-aggregate (for simplicity the noninteracting phenyl substituents are not shown).

TABLE 2: Investigated w_0 Values, Hydrodynamic Radii R_H, Depolarized RLS Ratio $\rho_V(90)$ at 500 nm, and Estimated Slip Angle φ and Aggregation Number N for the Various Microemulsions

w_0	R_H (Å)	$\rho v(90)$	φ (deg)	N
32	68	0.13	42	23
34	75	0.14	38	24
43	90	0.165	34	25
54	110	0.17	33	33
65	170	0.23	25	40

aggregate, we can estimate a number N ranging between 23 and 40 porphyrin units in the inner water compartments. The value obtained for $w_0 = 32$ ($N = 23$) is very close to the aggregation number for TPPS$_4$ J-aggregates as measured by previous QELS experiments.[23]

Exciton theory allows for a calculation of the spectroscopic aggregation number N_S, from the spectral width of the absorption band of the J-aggregate, which is proportional to $N_S^{-1/2}$.[41] To evaluate the effective bandwidth for absorption, the extinction spectra, as measured by a spectrophotometer, have to be corrected for the scattering component, which, close to the red portion of the 490 nm Soret band, is rather important. A dissection of scattering and absorption can be conveniently done by a simple method that is based on two independent measurements of extinction and RLS on the same sample and a linear regression analysis of the data in the region close to the resonance.[42]

An example of the procedure is reported in Figure 6, which shows the original extinction spectrum and the corrected one. The inset reports the linear fitting procedure of extinction versus RLS intensity in a properly chosen spectral region (in the red
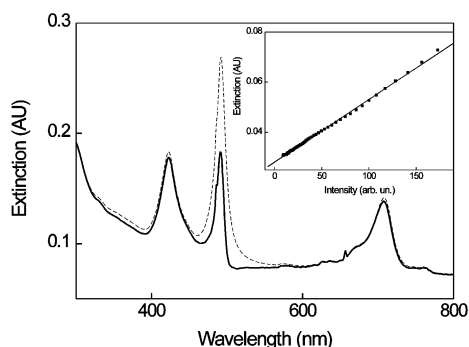
Figure 6. Extinction spectrum of a sample of J-aggregated TPPS$_4$ in AOT microemulsions (dotted line). Absorption spectrum after the correction from the scattering component (solid line). The inset reports the linear regression between the extinction and the RLS intensity data in the spectral region 500–570 nm. Experimental conditions: $w_0 = 65$, [TPPS$_4$] = 40 μM, in 25 mM citrate buffer at pH 2.7, $T = 293$ K.

edge portion of the absorption band). This method gives us an estimate of the full width at half-maximum (fwhm), and consequently the corresponding values of the spectroscopic aggregation numbers N_S for the J-aggregates in the microemulsions at different w_0. To apply the method of the spectral narrowing, a value of 875 cm^{-1} has been used as the fwhm value for the monomer band (the Soret band of the diacid porphyrin at 434 nm). Assuming the model recently proposed in the literature[22] in which the porphyrins form monodimensional arrays, and considering the radius of a single molecule close to 1 nm, we can calculate the coherence length L as ($N_S + 1$) times the radius of a single porphyrin. The ratio R between the coherence length and the spectroscopic aggregation number indicates the quality of the exciton delocalization, being close to unity for an ideal J-aggregate. The maximum value for this parameter reported so far has been 0.25, for J-aggregates obtained in acidic aqueous solutions, using ammonium chloride as the nucleating agent.[22] Interestingly, the R values obtained in the present case range between 1.08 and 0.35 for the smallest ($w_0 = 32$) and the largest ($w_0 = 65$) microemulsions, respectively, suggesting a high level of coherence for these aggregates.

Concluding Remarks

The observation of a threshold size for the formation of the J-band suggests that the aggregation is preceded by a nucleation phase, in which the formation of seeds having a minimum size of 2–3 porphyrin units is a prerequisite for the growth of the aggregates. This conclusion is consistent with a recent kinetic model proposed for such assembly processes, even if in bulk solution.[35,36] However, on the basis of our results, it is not possible to exclude that the absence of aggregation below a critical size is due to confinement effects on the reagents.

On the basis of the present results, we expect that, depending on the nature of the surfactant and the composition, microemulsions can be conveniently exploited in the formation of porphyrin J-aggregates, allowing a fine control of their dimensions. The high level of coherence measured in these nanoaggregates can be conveniently exploited for applications in nonlinear optics. The possibility of further tuning the photophysical properties of such aggregates through a chemical modulation of the porphyrins (peripheral substituent groups or inserted metal ions) opens the way to a large variety of applications in the nanoscale. Such studies are currently in progress in our laboratories.

References and Notes

(1) Bawendi, M. C.; Steigerwald, M. L.; Brus, L. E. *Annu. Rev. Phys. Chem.* **1990**, *41*, 477.

(2) Pasternack, R. F.; Gibbs, E. J. *Met. Ions Biol. Syst., Vol 33* **1996**, *33*, 367–397.

(3) White, W. I. In *The Porphyrins*; Dolphin, D., Ed.; Academic Press: New York, 1978; Vol. 5, p 303.

(4) Kano, H.; Saito, T.; Kobayashi, T. *J. Phys. Chem. B* **2001**, *105*, 413–419.

(5) Kano, H.; Kobayashi, T. *Bull. Chem. Soc. Jpn.* **2002**, *75*, 1071–1074.

(6) Kano, H.; Kobayashi, T. *J. Chem. Phys.* **2002**, *116*, 184–195.

(7) Ohno, O.; Kaizu, Y.; Kobayashi, H. *J. Chem. Phys.* **1993**, *99*, 4128–4139.

(8) Maiti, N. C.; Ravikanth, M.; Mazumdar, S.; Periasamy, N. *J. Phys. Chem.* **1995**, *99*, 17192–17197.

(9) Ribo, J. M.; Crusats, J.; Farrera, J. A.; Valero, M. L. *J. Chem. Soc., Chem. Commun.* **1994**, 681–682.

(10) Akins, D. L.; Zhu, H. R.; Guo, C. *J. Phys. Chem.* **1994**, *98*, 3612–3618.

(11) Pasternack, R. F.; Schaefer, K. F.; Hambright, P. *Inorg. Chem.* **1994**, *33*, 2062–2065.

(12) Akins, D. L.; Zhu, H. R.; Guo, C. *J. Phys. Chem.* **1996**, *100*, 5420–5425.

(13) Akins, D. L.; Ozcelik, S.; Zhu, H. R.; Guo, C. *J. Phys. Chem.* **1996**, *100*, 14390–14396.

(14) Collings, P. J.; Gibbs, E. J.; Starr, T. E.; Vafek, O.; Yee, C.; Pomerance, L. A.; Pasternack, R. F. *J. Phys. Chem. B* **1999**, *103*, 8474–8481.

(15) Gandini, S. C. M.; Yushmanov, V. E.; Borissevitch, I. E.; Tabak, M. *Langmuir* **1999**, *15*, 6233–6243.

(16) Micali, N.; Romeo, A.; Lauceri, R.; Purrello, R.; Mallamace, F.; Scolaro, L. M. *J. Phys. Chem. B* **2000**, *104*, 9416–9420.

(17) Paulo, P. M. R.; Costa, S. M. B. *Photochem. Photobiol. Sci.* **2003**, *2*, 597–604.

(18) Purrello, R.; Scolaro, L. M.; Bellacchio, E.; Gurrieri, S.; Romeo, A. *Inorg. Chem.* **1998**, *37*, 3647–3648.

(19) Pasternack, R. F.; Collings, P. J. *Science* **1995**, *269*, 935–939.

(20) Schwab, A. D.; Smith, D. E.; Rich, C. S.; Young, E. R.; Smith, W. F.; dePaula, J. C. *J. Phys. Chem. B* **2003**, *107*, 11339–11345.

(21) Rotomskis, R.; Augulis, R.; Snitka, V.; Valiokas, R.; Liedberg, B. *J. Phys. Chem. B* **2004**, *108*, 2833–2838.

(22) Koti, A. S. R.; Taneja, J.; Periasamy, N. *Chem. Phys. Lett.* **2003**, *375*, 171–176.

(23) Micali, N.; Mallamace, F.; Romeo, A.; Purrello, R.; Scolaro, L. M. *J. Phys. Chem. B* **2000**, *104*, 5897–5904.

(24) Castriciano, M.; Romeo, A.; Villari, V.; Micali, N.; Scolaro, L. M. *J. Phys. Chem. B* **2003**, *107*, 8765–8771.

(25) Robinson, B. H.; Khan-Lodhi, A. N.; Towey, T. In *Structure and reactivity in reverse micelles*; Pileni, M. P., Ed.; Elsevier: New York, 1989; Vol. 65, pp 198–220.

(26) Togashi, D. M.; Costa, S. M. B. *Phys. Chem. Chem. Phys.* **2002**, *2*, 5437–5444.

(27) Togashi, D. M.; Costa, S. M. B. *Phys. Chem. Chem. Phys.* **2002**, *4*, 1141–1150.

(28) Aoudia, M.; Rodgers, M. A. J. *J. Phys. Chem. B* **2003**, *107*, 6194–6207.

(29) Hauser, H.; Haering, G.; Pande, A.; Luisi, P. L. *J. Phys. Chem.* **1989**, *93*, 7869.

(30) Christopher, D. J.; Yarwood, J.; Belton, P. S.; Hills, B. P. *J. Colloid Interface Sci.* **1992**, *152*, 465.

(31) Onori, G.; Santucci, A. *J. Phys. Chem.* **1993**, *97*, 5430.

(32) Amico, P.; D'Angelo, M.; Onori, G.; Santucci, A. *Il Nuovo Cimento* **1995**, *17*, 1053.

(33) Parkash, J.; Robblee, J. H.; Agnew, J.; Gibbs, E.; Collings, P.; Pasternack, R. F.; de Paula, J. C. *Biophys. J.* **1998**, *74*, 2089–2099.

(34) Any attempt to isolate and concentrate the "filled" microemulsions from the empty ones by exploiting ultracentrifugation was unsuccessful, leading in most cases to large clusters. A possible explanation of this phenomenon can be based on the normal tendency of TPPS$_4$ J-aggregates to form higher aggregates, which is usually observed in aqueous solutions. When the microemulsions containing the nanoaggregates are fostered in a restricted volume by the centrifuge force, the consequential anomalous increase of the concentration of microemulsions leads to an efficient clustering process. A similar instability of these nanoaggregate systems has been observed on raising the temperature close to the percolative transition of the AOT/water/decane ternary system (see Cametti, C.; Codastefano, P.; Tartaglia, P.; Rouch, J.; Chen, S. H. *Phys. Rev. Lett.* **1990**, *64*, 1461–1464. Peyrelasse, J.; Boned, C. *Phys. Rev. A* **1990**, 41, 938–953. Hait, S. K.; Moulik, S. P.; Rodgers, M. P.; Burke, S. E.; Palepu, R. *J. Phys. Chem. B* **2001**, 105, 7145–7154).

(35) Pasternack, R. F.; Fleming, C.; Herring, S.; Collings, P. J.; dePaula, J.; DeCastro, G.; Gibbs, E. J. *Biophys. J.* **2000**, *79*, 550−560.

(36) Pasternack, R. F.; Gibbs, E. J.; Collings, P. J.; dePaula, J. C.; Turzo, L. C.; Terracina, A. *J. Am. Chem. Soc.* **1998**, *120*, 5873−5878.

(37) Leyvraz, F. In *On growth and Form*; Stanley, H. E., Ostrowski, N., Eds.; Martinus Nijhoff Publishers: Dordrecht, 1986; pp 136−144.

(38) Bagwe, R. P.; Khilar, K. C. *Langmuir* **1997**, *13*, 6432−6438.

(39) Agostiano, A.; Cosma, P.; Trotta, M.; Monsù Scolaro, L.; Micali, N. *J. Phys. Chem. B* **2002**, *106*, 12820−12829.

(40) Kano, K.; Fukuda, K.; Wakami, H.; Nishiyabu, R.; Pasternack, R. F. *J. Am. Chem. Soc.* **2000**, *122*, 7494−7502.

(41) Knapp, E. W. *Chem. Phys.* **1984**, *85*, 73.

(42) Micali, N.; Mallamace, F.; Castriciano, M.; Romeo, A.; Monsù Scolaro, L. *Anal. Chem.* **2001**, *73*, 4958−4963.